

Nickel oxide nanofibers manufactured via sol-gel method: synthesis, characterization and use it as a photo-anode in the dye sensitized solar cell

B. E. Jasim ^a, N. A. A. Aboud ^a, A. M. Rheima ^{b*}

^a*Department of Chemical Industrial, Institute of Technology, Baghdad, Middle Technical University, Iraq.*

^b*Department of Chemistry, College of Science, Mustansiriyah University, Baghdad, Iraq.*

A modified method with sol-gel nickel oxide (NiO) nano fibers was used for current research synthesized. FE- SEM, AFM, and UV visible spectroscopy were used to investigate the morphology and optic properties of the synthesized nano. The synthesized nickel oxide structure has been demonstrated with X-ray diffraction (XRD), average crystalline size was 10.08 nm while particle size ~23 nm with fiber structure from FE- SEM and 16.87 nm from AFM. Nanofiber was used to produce a new solar cell (ITO/ NiO/ Rhodamine 6 G/iodide/Al nanofilm/ITO) with a photo-sensitization of approximately 0.973%.

(Received September 8, 2021; Accepted January 18, 2022)

Keywords: Dye-sensitized solar cells, Sol-gel, NiO, Optical properties and Rhodamine 6 G

1. Introduction

Nanostructures have drawn considerable interest due to their unusual properties in different fields compared to their bulk counterparts[1][2]. Reducing the particle size to the nanometer scale results in a number of interesting properties relative to they have their bulk assets[3][4]. It has a large surface area and in many applications, metal oxide nanomaterials provide great advantages over conventional materials. Transparent semi-conductor material, effective as low cost thin films, is widely used in a broad range of applications, including Windows architectural [5], light transparent electrodes and solar cells [6][7] as well as many other optoelectronic tools.

Nano-sized NiO has shown outstanding features like electrochromic [8] catalytic[9], optical and electrochemical properties [10] magnetic [11]. In addition, nickel oxides can be used as a semi-conducting layer of transparent p-type [12]. Study of electrochemical smart windows applications super sensitivities [13] and photocathodes sensitized by dye [14][15]. Variety techniques for synthesis and modification were used for nanoscale nickel oxide, e.g. electrodeposition [16], evaporation[17], thermal decomposition [17] sputtering [18] and Sol-gel techniques [19][20]. Thermal decomposition process has some kind of benefits such as a quick method, low cost and ease of obtaining High purity products are thus very appealing and Industrial applications are simple to use.

In the last decades, a lot of efforts have been made to develop different forms of dye sensitizers, and the connection between the chemical structures and the photovoltaic performs of DSSCs has been accumulated over time, efficient organic dye to optimize chemical structures for good light-harvesting properties should be created, good electron contact between the dye and a NiO electrode should be provided [21]. In laser dye and DSSC [22], rhodamine 6G is good dye[23], the pigmentation consists of exceptionally high picture stability, high quantum fluorescence (0.95) in laser and low cost with efficiency in DSSC [24][25]. In this study, Nickel oxide nanofibers was synthesized by sol-gel and used as a photo-anode in the dye sensitized solar cell.

* Corresponding author: arahema@uowasit.edu.iq
<https://doi.org/10.15251/DJNB.2022.171.59>

2. Experimental

2.1. Synthesis of nickel oxide nanostructure

Using $[\text{Ni}(\text{CH}_3\text{COO})_2 \cdot 4\text{H}_2\text{O}]$ Nickel acetate tetrahydrate as a starting material, NiO was synthesized using the sol-gel process. 2 mmol of nickel acetate has been dissolved into 25 ml of 2-methoxyethanol solution starting (15 min) at room temperature then added to the sodium hydroxide solution. The molar ratio of sodium hydroxide solution to nickel acetate was kept at 2:1, PH was changed to (10.5) , the mixture obtained has been stirring at 50 °C for 3 h to produce a smooth and homogeneous gel substance, then a gel dried at 100 °C for 15 min in an oven to evaporate the solvent then calcinated at 450 °C for 3hs.

2.2. Photo-sensitized solar cell fabrication

Manufacturing of the ITO (Indium tin oxide coated glass) solar cell photo-sensitized, with 10 ohm resistant and 85% transmission properties cleaning with ethanol, deionized water several times in an ultrasound bath to remove the impurities.

Photo-sensitized solar cells with (1.5 * 2 * 0.1) cm were created using the following technique a colloidal solution of nanostructure has been blended with 0.3 g NiO nanopowder in the form of 5 ml of ethyl alcohol. The photoanode made with a dropper on the leading side of the glass with the colloidal solution then dry at 200°C, As the NiO nanostructure was cooled, it was submerged with 0.05 M (Rhodamine 6 G) overnight.

A conductive glass side electrode counter covers with aluminum nanofilm using Vacuum thermal evaporation chamber [26]. The (I/I^3) used as electrolyte solution was dropped into working area through capillary action seen between photoanode and the counter electrode. Both electrodes have been held together using binder clips

3. Results and discussions

3.1. Structural properties

3.1.1. X-ray diffraction (XRD)

The nanostructure x-ray diffraction form was investigated using (SHIMADZU XRD-6000), Figure(1) displays the NiO nanostructure (XRD) pattern, throughout this (XRD) data the observed indexed peaks are totally compatible with the corresponding pure cubic crystalline NiO. Several peaks in pattern at $2\theta = 37.19^\circ, 43.34^\circ, 62.74^\circ, 75.34^\circ$ and 79.86° assigned to (1 1 1), (2 0 0), (2 2 0), (3 1 1) and (2 2 2) crystallinity planes. The peaks indexed are entirely in accordance with the crystalline cubic ordered NiO (JCPDS 01-1239) [27]. Moreover, in the pattern that validate the crystalline with pure cubic phase no peaks for impurities such as $\text{Ni}(\text{OH})_2$ or other phases have been detected. Average crystall diameter (D) was (10.08) nm calculated with use of Scherrer formula [28]

$$D = k\lambda / \beta \cos \theta \quad (1)$$

where $k = 0.9$, $\lambda = (0.1406)$ represent the wavelength of X-rays used, $\beta =$ full width at half maximum (FWHM) and $\theta =$ angle of diffraction.

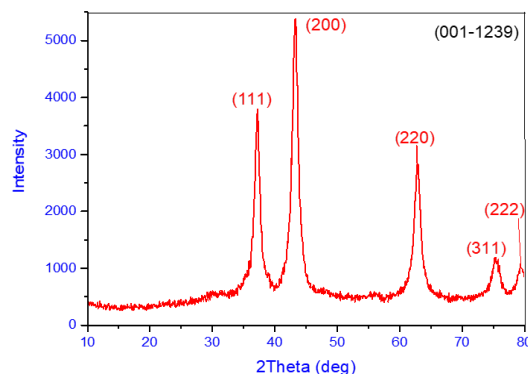


Fig. 1. XRD pattern of nickel oxide nanorods.

3.1.2 Field Emission scanning electron microscopy (FE-SEM)

The morphology of the surface of the synthesized nanorods (FE-SEM) was investigated in figure (2). From the micrograph it is evident that the fiber is extremely fine and there is tiny a nano assembly the average grain size was (~ 23 nm).

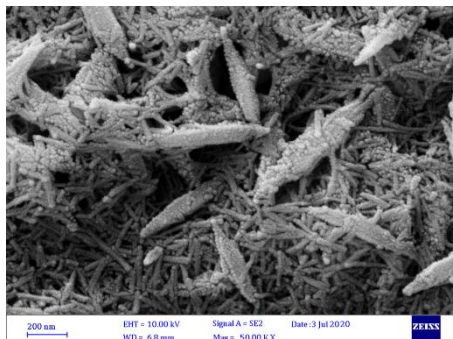


Fig. 2. FE-SEM image NiO nanofibers.

3.1.3. Atomic force microscopy (AFM)

Atomic force microscopy was used to depict surface morphology using (USA, Angstrom Advanced Inc., AA3000 model), the 3D image figure (3)(a) demonstrates a fiber with strong vertical order and varying degrees of surface homogeneity while figure (3)(b) describes a granularity distribution chart of nano nickel oxide with the minimum and maximum values of a granular size varying between (10-30) nm and the most significant percentage of nanofibers was $\leq 90\%$ Diameter: 13 nm. From AFM the average grain size was 16.87 nm.

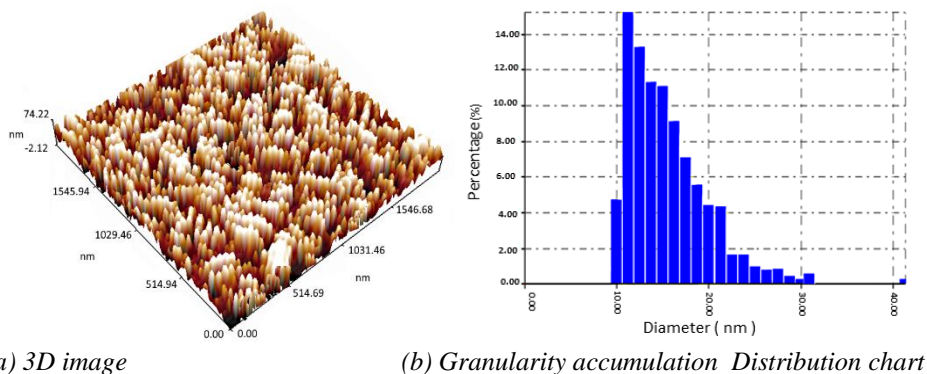


Fig. 3. AFM of nickel oxide nanostructure.

3.2. Optical properties

3.2.1. UV-VIS spectrophotometer

The UV-Vis spectrum ranged between 200 and 900 nm, using 1 cm quartz cells of the Shimadzu spectrophotometer. Figure (4-A) illustrates NiO spectrum with two peaks, the first peak with a high absorption due to electronic absorption of valence band while second broad peak as shoulder around (245 -260) nm due to oxygen- metal charge transfer excitation [29].

The Bandgap energy (E_g) is measured from UV-Vis data using taut plots, as seen in figure (4-B) by extrapolating the linear component of the curve (E_g) values represent as (3.92) eV. As compared the energy gap of experimental results nanostructure synthesized with the bulk NiO semiconductor ($E_g=3.74$ eV) varies energy gap due to the quantum confinement effects and the increasing surface to volume ratio [30].

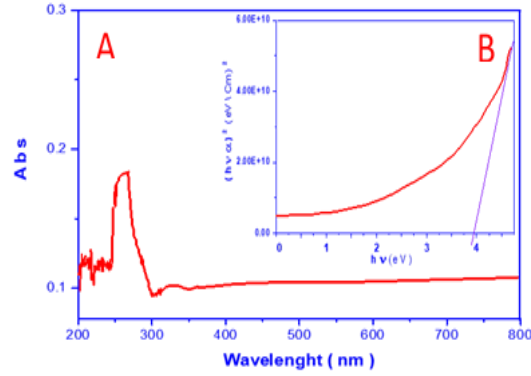


Fig. 4. (A) UV-vis absorption spectrum and (B) E_g (eV).

3.3. Photosensitized solar cell parameter

Cell parameters are seen in Figure (5); I_{sc} , V_{oc} , I_{max} and v_{max} have been estimated from the (I-V) curves; the solar simulator consists of a (100 mW/cm²) halogen lamp for solar cells. The energy conversion performance of the solar cells was calculated using the equation (2)

$$\eta = \frac{p_m}{p_{in}} * 100\% \quad E \quad (2)$$

where, p_m = maximum power , p_{in} = light power.

While (FF) as fill factor were calculated using the equations(3) [31-38]:

$$F.F = \frac{J_m * v_m}{J_{sc} * v_{oc}} \quad (3)$$

where, V_m = maximum output voltage , J_m = maximum current density, J_{sc} = shortcircuit current density and V_{oc} = open circuit voltage . The solar cell parameters are V_{oc} = 0.270 V, J_{sc} = 0.078 A/cm², V_{max} = 0.18 V, J_{max} = 0.054 A/cm² and FF = 0.458 with conversion efficiency 0.973%. The relative high parameters are observed in photo-solar cells attributable to the extremely surface area ratio as well as redox rate of electron diffusion. All parameters are shown in the Table 1.

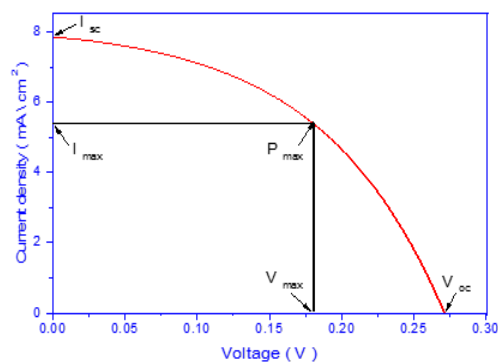


Fig. 5. DSSC photovoltaic properties.

Table 1. Illustrate the cells parameters of NiO.

DSSC					Voc (V)	J sc (A/cm ²)	V max (V)	J max (A/cm ²)	P max (W/cm ²)	FF	η %
	Nano	Anode	Cathode	dye							
1	NiO	ITO/ NiO	ITO/Ag	Rhodamine 6 G	0.270	0.078	0.18	0.054	0.0097	0.458	0.973

4. Conclusion

NiO nanofibers are the economically materials used in dye sensitized solar cells (DSSC). The nanofibers with dye (Rhodamine 6G) take on the role of light absorption and of transporting the chargers in DSSC. In our study the DSSC consists of NiO which are used to harvest sunlight with vast surfaces. The NiO was developed on ITO substrate and it was used as an electrode for the solar cell broad gap semi-conductor. Rhodamine 6G dye sensitized immersed with NiO electrodes. The effectiveness of using thin layer from NiO nanostructure as anode in DSSC gives a good efficiencies which directly affected the absorption of the dye on its surface also light absorption properties of Rhodamine 6 G have a maximum response throughout visible spectra. SEM was used to observe nanofibers of NiO and XRD was used to test their crystallinity. Due to the increased surface area from the nanostructure, which allows fast electron transmission through nanofibers, relative higher efficiency of DSSC was observed as 0.973 %.

References

- [1] N. A. Aboud, W. M. S. Alkayat, D. H. Hussain, *Drug Invent. Today* 13(3), 81 (2020).
- [2] A. H. Ismail, Z. S. Abbas, A. M. Rheima, *J. Xi'an Univ. Archit. Technol.* 12(2), 1 (2020); <https://doi.org/10.5101/nbe.v12i2.p139-147>
- [3] A. M. Rheima, R. S. Mahmood, D. H. Hussain, Z. S. Abbas, *Digest Journal of Nanomaterials and Biostructures* 15(4), 2020.
- [4] N. A. A. Aboud, W. M. S. Alkayat, D. H. Hussain, *Syst. Rev. Pharm.* 11(6), 1188 (2020).
- [5] N. A. Aboud, B. E. Jasim, A. M. Rheima, *Chalcogenide Letters* 18(5), 237 (2021).
- [6] A. M. Rheima, M. A. Mohammed, S. H. Jaber et al., *Desalination and Water Treatment* 194, 187 (2020); <https://doi.org/10.5004/dwt.2020.25846>
- [7] N. Abdul-Ameer Aboud, W. M. S. Alkayat, D. H. Hussain, *J. Phys. Conf. Ser.* 1664(1), 0 (2020); <https://doi.org/10.1088/1742-6596/1664/1/012116>
- [8] A. H. Ismail, H. K. Al-Bairmani, Z. S. Abbas et al., *Nano Biomed. Eng.* 12(2), 139 (2020); <https://doi.org/10.5101/nbe.v12i2.p139-147>
- [9] A. M. Rheima, N. A. Aboud, B. E. Jasim, A. H. Ismail, Z. S. Abbas, *International journal of pharmaceutical research* 13(1), 342 (2021).
- [10] A. Rheima, A. A. Anber, A. Shakir, A. Salah Hamed, S. Hameed. *Iranian Journal of Physics Research* 20(3), 51 (2020)
- [11] A. M. Rheima, A. A. Anber, H. I. Abdullah, A. H. Ismail, *Nano Biomed. Eng.* 13(1), 1 (2021); <https://doi.org/10.5101/nbe.v13i1.p1-5>
- [12] S.H. Mohammed, A. Rheima, F. Al-jaafari, M. F. Al-Marjani, Z. S. Abbas. *Egyptian Journal of Chemistry.* 2021 Oct 24.
- [13] A. F. Kamil, H. I. Abdullah, A. M. Rheima, S. H. Mohammed, *Egyptian Journal of Chemistry*, 64 (11) 6137, 2021.
- [14] M. Bonomo, D. Di Girolamo, M. Piccinni, *Nanomaterials* 10(1), 2020; <https://doi.org/10.3390/nano10010167>
- [15] A. M. Rheima, D. H. Hussain, H. I. Abdullah, *Silver nanoparticles : Synthesis , Characterization and their used a counter electrodes in novel Dye sensitizer solar cell* 9(10), (6) 2016.
- [16] I. Saadeddin, M. Suleiman, A. Rougier, *Solid State Ionics* 343, 115129 (2019); <https://doi.org/10.1016/j.ssi.2019.115129>
- [17] D. Wu, C. Zhuang, Z. Sun, *J. Mater. Chem. A* 7(14), 8485 (2019); <https://doi.org/10.1039/C9TA00529C>
- [18] Y. Xia, Y. Zeng, Y. Zhao, *J. Solid State Chem.* 269, 132 (2019); <https://doi.org/10.1016/j.jssc.2018.09.024>
- [19] S. Esposito, *Materials* 12(4), 1 (2019); <https://doi.org/10.3390/ma12040668>

- [20] A. A. Al-Ghamdi, W. E. Mahmoud, S. J. Yagmour, *J. Alloys Compd.* 486(1-2), 9 (2009); <https://doi.org/10.1016/j.jallcom.2009.06.139>
- [21] Y. Ooyama, Y. Harima, *European J. Org. Chem.* 18, 2903 (2009); <https://doi.org/10.1002/ejoc.200900236>
- [22] D. H. Hussain, H. I. Abdullah, A. M. Rheima, *Int. J. Sci. Res. Publ.* 6(10), 26 (2016).
- [23] S. Rani, P. K. Shishodia, R. M. Mehra, *J. Renew. Sustain. Energy* 2(4), 2010; <https://doi.org/10.1063/1.3463056>
- [24] W. K. A. Suhad Hassan Mohsen, Luma Hafedh Abed Oneizah, *J. Southwest Jiaotong Univ.* 54(4), 1 (2019).
- [25] R. F. Kubin, A. N. Fletcher, *J. Lumin.* 27(4), 455 (1982); [https://doi.org/10.1016/0022-2313\(82\)90045-X](https://doi.org/10.1016/0022-2313(82)90045-X)
- [26] R. J. Martín-Palma, A. Lakhtakia, *Vapor-Deposition Techniques*. Elsevier Inc., 2013; <https://doi.org/10.1016/B978-0-12-415995-2.00015-5>
- [27] M. R. Kalaie, A. A. Youzbashi, M. A. Meshkot, F. Hosseini-Nasab, *Appl. Nanosci.* 6(6), 789 (2016); <https://doi.org/10.1007/s13204-015-0498-3>
- [28] A. S. Vorokh, *Nanosyst. Physics, Chem. Math.* 9(3), 364 (2018); <https://doi.org/10.17586/2220-8054-2018-9-3-364-369>
- [29] U. Riaz, S. M. Ashraf, T. Fatima, S. Jadoun, *Spectrochim. Acta - Part A Mol. Biomol. Spectrosc.* 173, 986 (2017); <https://doi.org/10.1016/j.saa.2016.11.003>
- [30] M. Nowsath Rifaya, T. Theivasanthi, M. Alagar, *Nanosci. Nanotechnol.* 2(5), 134 (2012); <https://doi.org/10.5923/j.nn.20120205.01>
- [31] A. Mahdi Rheima, D. Hadi Hussain, H. Jawad Abed, *IOP Conf. Ser. Mater. Sci. Eng.* 928(5), 2020; <https://doi.org/10.1088/1757-899X/928/5/052036>
- [32] A. F. Kamil, H. I. Abdullah, A. M. Rheima, S. H. Mohammed, *Journal of Ovonic Research* 17(3), 253 (2021).
- [33] A. F. Kamil, H. I. Abdullah, A. M. Rheima, S. H. Mohammed. *Materials Today: Proceedings*. 2021 Oct 21.
- [34] A. F. Kamil, H. I. Abdullah, A. M. Rheima, S. H. Mohammed. *Materials Today: Proceedings*. 2021 Oct 7.
- [35] A. F. Kamil, H. I. Abdullah, A. M. Rheima, S. H. Mohammed, S. J. Tumaa , R. M. Abed. *Digest Journal of Nanomaterials & Biostructures*, 16(4), 1453 (2021).
- [36] A. F. Kamil, H. I. Abdullah, A. M. Rheima, WM Khamis, *Journal of Ovonic Research* ,17(3), 299 (2021).
- [37] H. A. Kadhum, W. M. Salih, A. M. Rheima, *Applied Physics A* 126(10), 1 (2020); <https://doi.org/10.1007/s00339-020-03985-6>
- [38] A. T. Salman, A.H. Ismail, A.M. Rheima, A.N. Abd, N.F. Habubi, Z.S. Abbas. In *Journal of Physics: Conference Series* 2021 Mar 1 (Vol. 1853, No. 1, p. 012021). IOP Publishing; <https://doi.org/10.1088/1742-6596/1853/1/012021>